ACS OMEGA

Article

Cite This: ACS Omega 2018, 3, 10851−10857

http://pubs.acs.org/journal/acsodf

Ag Nanometallic Surfaces for Self-Assembled Ordered Morphologies of Zein

Apoorva Gurtu and Mandeep Singh Bakshi*

Department of Natural and Applied Sciences, University of Wisconsin—Green Bay, 2420 Nicolet Drive, Green Bay, Wisconsin 54311-7001, United States

Supporting Information

ABSTRACT: Nanometallic surfaces of Ag nanoparticles (NPs) catalyzed the self-aggregation behavior of zein in different ordered morphologies such as cubes, rectangles, and bars. This was studied in a ternary in situ reaction ($AgNO_3$ + zein + water), where zein performed the reduction as well as stabilization of Ag NPs. This reaction produced small Ag NPs of less than 10 nm predominantly bound with {111} crystal planes, which attracted the surface adsorption of zein. Surface-adsorbed zein initiated the protein seeding and converted the tertiary structure of protein into open β-pleated structure with aqueous exposed hydrophobic domains. A layered deposition of β-pleats on different crystal planes of Ag NPs derived them to nearly monodispersed cubic morphologies. The mechanistic aspects of self-aggregation of zein in the presence of nanometallic surfaces hold possible scenarios for simple and straightforward routes of protein crystallization.

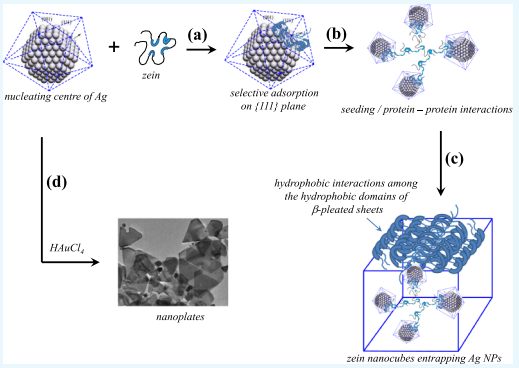

INTRODUCTION

Protein crystallization is an important aspect to understand the structural and site specific biochemical reactions. It is usually carried out in the aqueous phase with precise control of the ionic strength, pH, temperature, and purity of the protein.[1−3] Because protein is a macromolecule and its physiochemical properties are highly protein-specific, a precise crystallization is quite tedious and requires a control over wide range of experimental conditions. Conventional protein crystallization is generally reported at the micrometer or millimeter scale but it can be controlled at the nanometer scale by generating suitable reaction conditions. Nanometallic surfaces with specific crystal planes of small metallic nucleating centers can be used to drive the ordered self-aggregation (that eventually leads to crystallization) of proteins.[4−7] A protein macromolecule is a complex entity consisting of hydrophilic and hydrophobic domains and hence prone to undergo various specific and nonspecific interactions with free surfaces.[8−10] This process causes several conformational changes in protein structure that eventually results in protein unfolding and exposes hydrophobic domains to aqueous phase. It triggers protein−protein interactions through seeding that leads to the onset of self-aggregation.[11−14] This complex process is little understood and requires a proper mechanistic approach to understand. It is particularly more prevalent in predominantly water-insoluble or hydrophobic proteins which contain high proportions of nonpolar amino acids. Thus, unraveling the mechanisms of protein in self-assembled ordered morphologies may help us to understand several complex scenarios associated about fibrillation as well as amyloidosis mainly responsible for Alzheimer's and Parkinson's diseases.

Zein, a corn-starch well-studied protein, is one of the common example of hydrophobic proteins that is available in plenty with a wide range of food and pharmaceutical applications. The hydrophobic nature of zein is mainly due to the presence of leucine, alanine, and proline that render it water-insoluble.[15,16] It is categorized into four different classes viz. α, β, γ, and δ based on its solubility, amino acid sequences, and surface charges. α-Zein[17] with molecular mass of 21−25 kD is the most abundant fraction and also contains large amounts of hydrophobic residues. We present a simple and straight forward method of nanometallic-catalyzed self-aggregation of zein in nanocube formation specifically in the presence of Ag nanoparticles (NPs). The main objective of the study is to elucidate the mechanism that how nanometallic surfaces and crystal structure[18,19] promote the ordered self-aggregation of proteins in shape-controlled morphologies with relevance to fibrillation with significant implications in nanomedicine.

RESULTS AND DISCUSSION

In Situ Synthesis of Zein Nanocubes. *In the Presence of Ag NPs.* Table 1 lists different conditions under which zein nanocubes are synthesized. Figure 1a shows the scanning electron microscopy (SEM) image of nanocubes of sample NC1 of ∼200 nm in size while the corresponding transmission electron microscope (TEM) image is shown in Figure 1b. The overall morphology of the nanocube is depicted by choosing

Received: August 17, 2018
Accepted: August 27, 2018
Published: September 7, 2018

DOI: 10.1021/acsomega.8b02086
ACS Omega 2018, 3, 10851−10857

Table 1. Chemical Composition Ternary in Situ Reaction, Final Color, Size, and Zeta Potential of Nanomorphologies[a]

sample	[$AgNO_3$]/mM	[zein]/% w/w	[SDS]/mM	final color	size/nm	zeta potential/mV
NC1	1.5	0.3	8	light yellow	~200	−41
NC2	1.5	0.3	16	yellow	~250	−47
NC3	1.5	0.4	20	dark yellow	~250	−57

[a]Zein solution is prepared in aqueous SDS solution.

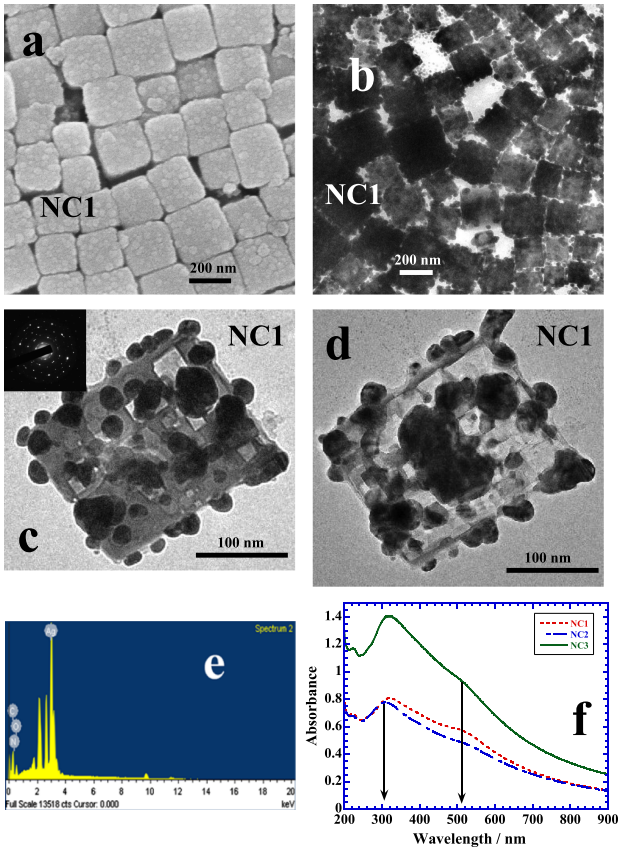

Figure 1. (a−d) SEM and TEM images of zein nanocubes entrapping small Ag NPs of sample NC1 (see Table 1 for chemical composition). EDX analysis (e) and UV−visible scans (f) of the samples.

two TEM images of single nanocube in Figure 1c,d. In both cases, Ag NPs are fully embedded in zein cubes and arranged in a random fashion with overall size ~10 nm while some of the NPs appear merging with each other. The selected area diffraction image in the inset of Figure 1c highlights the crystalline nature of Ag NPs. Energy dispersive X-rays (EDX) analysis of zein nanocubes show a prominent emission because of Ag apart from C, N, and O, the main elements of protein structure (Figure 1e). Figure 1f depicts the UV−visible plots of NC1, NC2, and NC3 samples (Table 1). The peak close to 300 nm is probably originating from the self-assembled zein while that at 510 nm is of immobilized Ag NPs in zein cubes. Free Ag NPs in aqueous solution usually give absorbance because of surface plasmon resonance (SPR) close to 410 nm.[20] There is practically no change in the position of SPR at 510 nm of entrapped Ag NPs while the peak at 300 nm red shifts ~15 nm with the increase in the amount of zein from 0.3 to 0.4%. Sample NC1 is prepared when zein is solubilized in 8 mM sodium dodecyl sulfate (SDS) which is the critical micelle concentration.[21] Increase in the amount of SDS from 8 to 16 and then 20 mM further facilitates the solubilization of zein by imparting greater degree of unfolding.[22] In other words, the degree of unfolding is related to the amount of surfactant used. Figure 2a,b shows the SEM images of samples NC2 and NC3

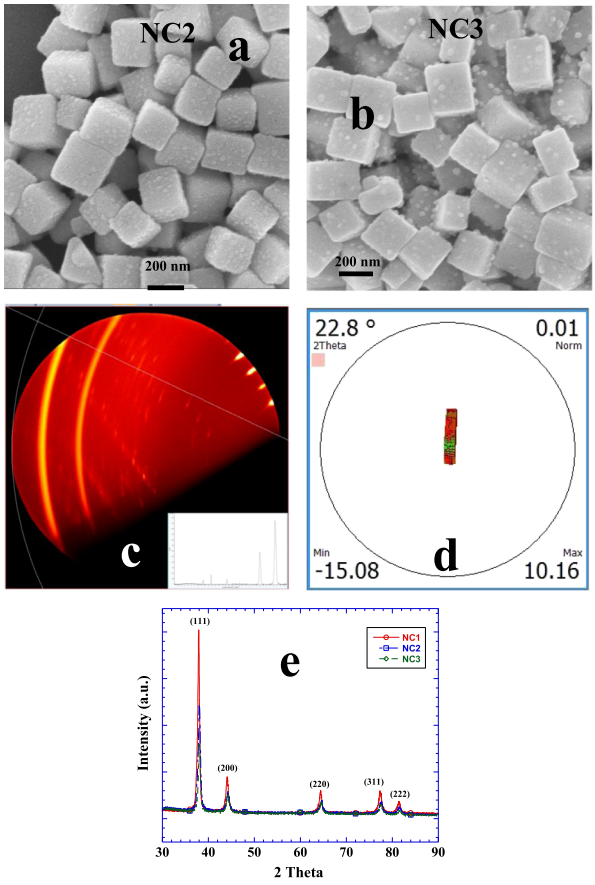

Figure 2. (a,b) SEM images of nanocubes of sample NC2 and NC3, respectively, (see Table 1 for chemical composition). (c) 2D XRD patterns and integrated plot (inset). (d) Texture map showing one family plane is parallel to the surface. (e) XRD patterns of Ag NPs of different samples showing the typical fcc geometry.

prepared by using 16 and 20 mM of SDS, respectively. Both images show almost identical morphologies with similar sizes. The sample specifications, size, and shape of all samples made under in situ experimental conditions have been listed in Table 1. Microscopic imaging data have been further compared with that from dynamic light scattering (DLS) measurements. There is a fine correlation between the size evaluated from the TEM (Table 1) and DLS (Figure S3) analysis. The zeta potential of nanocubes from different samples is negative (Figure S4) and in the range of ~(−40 to −60) mV. Negative zeta potential is obviously due to the global negative charge on zein dissolved in aqueous SDS.[22] 2D X-ray diffraction (XRD) analysis further helps us to elucidate the ordered self-aggregation of zein. Here is a composite of many scans at 2 theta equal 20 and psi 57° as the sample is rotated (Figure 2c). The spots are from protein, with the bright ones in the upper

DOI: 10.1021/acsomega.8b02086
ACS Omega 2018, 3, 10851−10857

Table 2. Chemical Composition in Situ Reaction, Final Color, and Size of Nanomorphologies[a]

sample	$[AgNO_3]$/mM	$[HAuCl_4]$/mM	[zein]/% w/w	[SDS]/mM	final color	size/nm
NC4	1.25	0.25	0.4	20	dark purple	∼400−1000
NC5	1.50	0.25	0.4	20	dark purple	∼400−1000

[a]Zein solution is prepared in aqueous SDS solution.

right nearly along the normal direction of the protean plane in contact with the sample along with an integrated 2D plot (Figure 2c, inset). Texture map (Figure 2d) from a series of scans rocking through a specular reflection of 2 theta equal to 22.8° shows that one family of protein planes is parallel to the surface. The crystal structure of Ag NPs shows the face-centered cubic lattice of Ag NPs (Figure 2e) with predominant growth at the {111} crystal planes. It suggests that {111} crystal planes are in fact nanometallic surfaces which promote the self-aggregation of zein.

Using Both $AgNO_3$ and $HAuCl_4$. Interestingly, when the above-mentioned in situ reaction in the presence of $AgNO_3$ is conducted along with a small amount (0.25 mM) of $HAuCl_4$ (Table 2), the monodisperse shape of nanocubes observed previously is largely disturbed with much larger sizes and appearance of different shapes such as bars, rectangles, and other less prominent polyhedral morphologies (Figure 3).

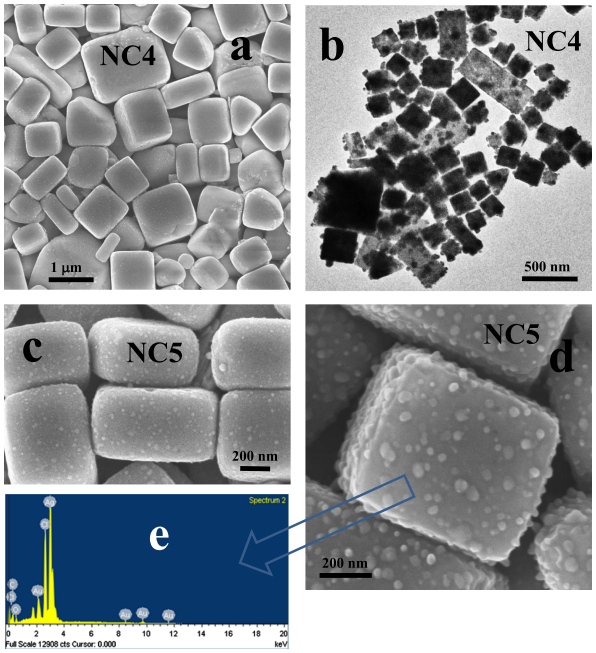

Figure 3. (a,b) SEM and TEM images of sample NC4 and (c,d) NC5 (see Table 2 for chemical composition). (e) EDX analysis of sample NC5.

Now, zein also reduces Au(III) into Au(0) along with the reduction of Ag(I) into Ag(0). As both reduction

$$x\mathrm{Ag}_{(aq)}^{+} + y\mathrm{Ag}_{(aq)}^{3+} + \text{zein protein (aq)} + (x+y)\mathrm{e}^{-} \rightarrow (x+y)(\mathrm{Ag}^{0} - \mathrm{Au}^{0})_{(s)} + \text{oxidizing products}$$

reactions are occurring simultaneously due to the weak reducing ability of zein, nucleating centers created in this way are the mixtures of both Ag and Au atoms with face-centered cubic (fcc) geometry.[23,24] They have different catalytic behavior[25,26] from Ag NPs that leads to the formation of rectangles, bars, and distorted tetrahedrons. In addition, there is a large variation in the size and shape of nanocubes and now nanocubes of more than 1 μm are also present. Apart from the self-assembled morphologies of zein, the reaction produces free Ag−Au bimetallic triangular planar NPs of 200−300 nm in the solution (Figures S5 and S6), which are not entrapped in zein nanocubes or any way associated with the self-assembled zein. They are responsible for the dark purple color of the solution (Table 2) in comparison to light yellow obtained only in the presence of Ag NPs (which are completely entrapped by the nanocubes) (Table 1). Large nanocubes and rectangles entrapping small NPs are shown in Figure 3c,d for the samples NC5 and NC6, respectively, while the EDX analysis is shown in Figure 3e. EDX analysis show prominent emission from Ag while relatively much weaker emission is coming from Au, along with that of Cl which is the byproduct of $HAuCl_4$.[27] We will elaborate it further from the detailed EDX analysis.

Using the Seed-Growth (S-G) Method to Produce NPs. In the S-G method, seeds are first prepared and then are subjected to growth conditions.[18,19] Growth is the process where shape and size are governed by the stabilizing agent that results in specific-shaped NPs with specific crystal planes.[18] Seeds are practically small NPs usually of ∼10 nm in size (Figures S1 and S2). Freshly produced atoms during the reduction reaction prefer to nucleate at the specific crystal planes of seeds already present in the solution rather than generating new nucleating centers.[18] Therefore, different crystal planes of growing seeds now provide the nanometallic surface catalytic effects and hence provide entirely different route of mechanism of self-assembled behavior of zein. We use both Au and Ag seeds in different growth steps with a fixed amount of $AgNO_3$ as precursor in the presence of zein (Table 3). During the growth reaction, again zein initiates the

Table 3. Chemical Composition Seed Growth in Situ Reaction, Final Color, and Size of Nanomorphologies[a]

sample	Au seeds/mM	$[AgNO_3]$/mM	[zein]/% w/w	[SDS]/mM	final color	size/nm
NC6	0.005	1.5	0.4	20	Brick red	∼300
NC7	0.01	1.5	0.4	20	Brick red	∼300
sample	Ag seeds/mM	$[AgNO_3]$/mM	[zein]/% w/w	[SDS]/mM	final color	size/nm
NC8	0.005	1.5	0.4	20	Brick red	∼300
NC9	0.01	1.5	0.4	20	Brick red	∼300

[a]Zein solution is prepared in aqueous SDS solution.

DOI: 10.1021/acsomega.8b02086
ACS Omega 2018, 3, 10851−10857

reduction of Ag(I) to produce Ag(0) which nucleates on different crystal planes of seeds to produce Ag−Au bimetallic NPs. The nanometallic surfaces of bimetallic NPs may further catalyze the self-aggregation of zein. Figure 4 shows the SEM

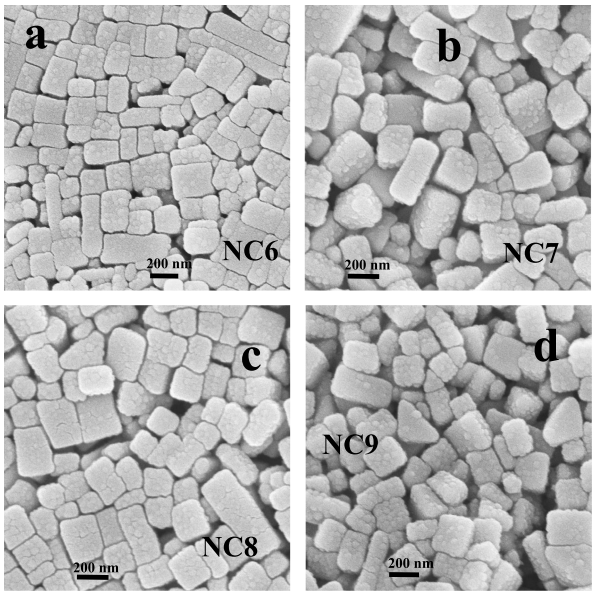

Figure 4. (a−d) SEM images of samples NC6 to NC9, respectively (see Table 3 for chemical composition).

images of zein self-assembled morphologies of samples NC7−NC10 (Table 3), while their respective TEM images are shown in Figures S7 and S8. Among various shapes, predominant morphologies are cubes, rectangles, and bars, as observed previously (Figure 3) for the samples of Table 2, where both $AgNO_3$ and $HAuCl_4$ are used. The main difference between the morphologies of samples of Tables 2 and 3 is the size, which is much larger (∼1 μM) for the samples of Table 2 rather than that (∼300 nm) of Table 3. This suggests that the NPs synthesized without the S-G method produce much bigger zein morphologies rather than with the S-G method.

Compositional Analysis. C, N, and O, are the main elements constituting the protein structure and contributing to maximum amount in each case (Table 4). Samples NC1−NC3 (Table 1) apart from these elements also show the presence of large amount of Ag in the form of Ag NPs. Therefore, the nanocubes of Figures 1 and 2 are mainly consisting of these elements. When we use both $AgNO_3$ and $HAuCl_4$ along with zein (samples NC4 and NC5, Table 2), the nanocubes (Figure 3) are mainly made of Ag (43.4%) while the amount of Au (1.4%) is too tiny in contrast to the bulk mole ratio 1:5 between Ag and Au. Presence of 9.7% Cl is the byproduct of $HAuCl_4$ ($AuCl \rightarrow 2Au + Cl_2$)[27] and is expected to form AgCl that may also exist in the form of nanocubes with almost similar dimensions.[28−30] On the other hand, the amount of Cl (1.4%) produced is almost negligible when Au seeds and $AgNO_3$ are used in the presence of zein (samples NC6 and NC7, Table 3). This tiny amount of Cl is probably contributed[27] by an unreacted $HAuCl_4$ during the synthesis of Au seeds. In fact, the NPs entrapped in the nanocubes of samples NC6 and NC7 (Figure 4) are mainly made of Ag, whereas amount of Au is almost negligible. Likewise, Ag seeds along with $AgNO_3$ and in the presence of zein (samples NC8 and NC9, Table 3) should produce only Ag NPs from the S-G method. Thus, elemental composition of all samples indicates that the nanocubes are mainly made of zein along with Ag NPs but also contain AgCl when $HAuCl_4$ is used and the amount of AgCl is proportional to the amount of Cl produced upon the decomposition of $HAuCl_4$. In addition, only the nanometallic surfaces or crystal planes of Ag NPs catalyze the self-aggregation of zein even in the samples NC4−NC7, where Au is used either in the form of $HAuCl_4$ or Au seeds. Hence, all results lead to an overall single mechanism of the nanocube formation under different conditions where only Ag nanometallic surfaces are involved in the self-aggregation of zein. In addition, the overall composition of zein in terms of C, N, and O is also largely affected because of the reaction conditions demonstrated in Table 1, which dramatically alter the zein tertiary structure. Surface adsorption of zein under different experimental conditions also alters the seeding process that in turn causes a large change in the protein composition.

Table 4. Chemical Composition in Atomic % of Zein Nanocubes Determined from the EDX Analysis

samples	C	N	O	Ag	Au	Cl
NC1	36.7	21.3	17.1	24.9		
NC2	40.4	37.9	10.6	11.1		
NC3	42.0	34.6	16.7	10.1		
average	39.7	24.3	14.8	15.4		
NC4	18.6	14.0	11.5	44.7	1.1	10.1
NC5	19.1	16.6	10.4	43.0	1.6	9.3
average	18.8	15.3	10.9	43.8	1.3	9.7
NC6	32.9	34.3	13.7	18.2	0.15	1.4
NC7	32.9	33.1	12.9	19.3	0.1	1.7
average	32.9	34.3	13.7	18.2	0.15	1.4
NC8	42.1	23.7	20.5	13.7		
NC9	40.3	25.0	19.6	15.1		
average	41.2	24.3	20.0	14.4		

Mechanism. The mechanism of nanocube formation consists of two main steps (Figure 5). In the first step, Ag NPs are formed, and in the second step, their nanometallic surfaces are involved in the ordered self-aggregation of zein. Without the first step, the second step cannot go ahead at its own because blank experiments without the presence of $AgNO_3$ do not show any self-aggregation of zein. XRD patterns of Ag NPs (Figure 2c) confirm the fcc geometry with preferential growth along the ⟨111⟩ zone in the first step. Because the reaction is only a ternary reaction with three components that is zein + $AgNO_3$ + water, the growth of the NPs is controlled by the solubilized zein which is negatively charged because neutral zein is predominantly hydrophobic water-insoluble protein and hence can only be dissolved in aqueous surfactant solution. Anionic SDS micellar solution provides net negative charge to zein because long hydrocarbon chains of the surfactant molecules penetrate into the cylindrical hydrophobic domains[10] while anionic surfactant head groups remain at the surface of zein for aqueous solubilization. As a whole, solubilized zein protein becomes an amphiphilic entity with negative charges at the surface while hydrophobic domains are hidden inside (Figure 5a). The amphiphilic protein is highly susceptible for the surface adsorption that is mainly driven by low lattice energy of the NP surface.[31−33] Adsorption on the low energy {111} crystal planes brings unfolding (Figure 5b) and further increases the surface adsorption that does not remain limited to that of {111} crystal planes because unfolded zein with exposed hydrophobic

DOI: 10.1021/acsomega.8b02086
ACS Omega 2018, 3, 10851−10857

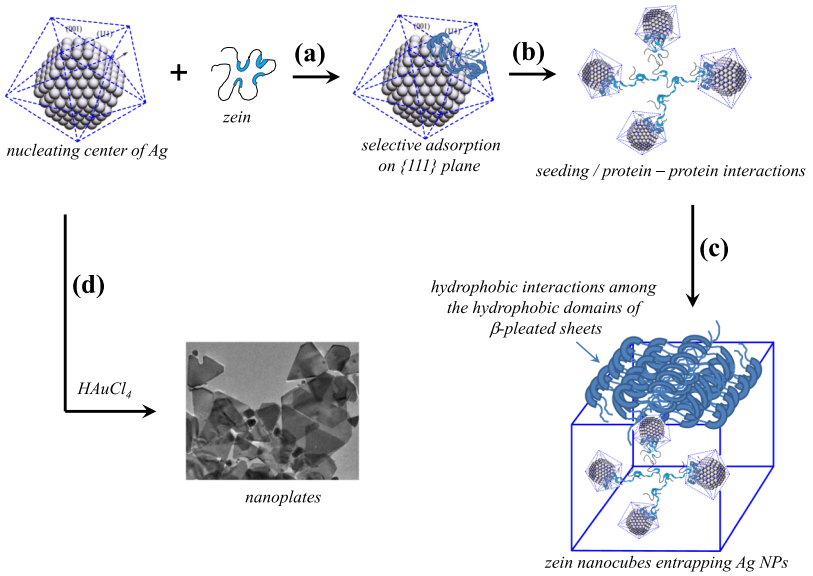

Figure 5. (a–d) Different steps of proposed mechanism of zein nanocube formation.

domains prefers to adsorb on {110}/{100} crystal planes.[8,10] Thus, nanometallic surface-adsorbed hydrophobic domains undergo hydrophobic interactions with aqueous solubilized free zein as well as with the surface-adsorbed zein on the neighboring NPs.[8] Such protein–protein interactions bring several layers of zein deposition on the nanometallic surfaces (Figure 5c). High temperature (80 °C) for 24 h in fact induces further dehydration to the hydrophobic domains and increases the magnitude of nonpolar interactions. Zein is a highly robust protein with cylindrical hydrophobic domains. Surface adsorption opens the cylindrical hydrophobic domains with layers of β-pleated sheets[34,35] that contain predominantly nonpolar amino acids. In fact, cubic morphologies are the outcome of β-pleated layered packing around each NP which then acts as a seed or nucleating center for the self-aggregation of zein.[10] When several adjoining NPs wrapped with β-pleated sheets make small aggregates driven by the hydrophobic interactions, a self-assembled cubic morphology of zein entrapping Ag NPs emerges. The shape and size of the final morphology is the result that how β-pleated sheets are packed around each NP.

Use of $HAuCl_4$ along with $AgNO_3$ in this reaction initiates other side reactions apart from the synthesis of Ag nucleating centers. Ag^+ ions interact electrostatically with negatively charged zein and hence preferentially reduced in comparison to $AuCl_4^-$ ions. Ag nucleating centers thus-produced follow the same mechanism as discussed above and result in the formation of Ag NPs entrapped zein nanocubes. These nanocubes indicate the presence of a little amount of Au (Table 4), suggesting a parallel growth of Ag–Au bimetallic nucleating centers into large nanoplates[36,37] (~200 nm, Figures S5 and S6), which do not entrap in the zein nanocubes. Rather their flat surfaces bound with {110}/{100} crystal planes are the ideal nanometallic surfaces for the adsorption of hydrophobic domains. It further opens and facilitates the layering of the β-pleated sheets that self-assemble into much larger rectangles and bars along with cubes (Figure 3).[38−40] Furthermore, use of Au seeds (Table 3, samples NC6 and NC7) even does not help to produce Ag–Au bimetallic NPs embedded in zein nanocubes because again a little amount of Au is present in nanocubes while all entrapped NPs are only made of Ag (Table 4). Thus, self-assembled behavior of zein is primarily originating from the Ag nanometallic surfaces and that is why the resulting zein nanocubes only contain Ag NPs rather than Ag–Au bimetallic or Au NPs. The formation of rectangles and bars are the manifestation of β-pleated sheet self-aggregation behavior when a large amount of zein is surface-adsorbed.

CONCLUDING REMARKS

Ag nanometallic surfaces demonstrate their excellent potential for the surface adsorption and self-aggregation behavior of zein in ordered morphologies. This is mainly achieved for predominantly hydrophobic proteins such as zein, while other predominantly hydrophilic proteins rarely show this behavior.[41−43] In situ reaction conditions are the best suited for the formation of monodisperse zein nanocubes when Ag nucleating centers are created during the reaction and that allow simultaneous preferential adsorption of zein on {111} crystal planes. It initiates the seeding and protein–protein interactions to deposit unfolded β-pleated layered structures on nanometallic surfaces to generate ordered morphologies. Zein nanocubes entrap only Ag NPs and do not entrap Ag–Au bimetallic NPs, indicating the fact that Ag nanometallic surfaces are preferred over bimetallic. This is most probably due to a change in the lattice structure which is probably not that favorable for the surface adsorption of zein in comparison to Ag nanometallic surface and requires further investigation.

EXPERIMENTAL

Chemicals. Zein protein (CAS # 9010-66-6), hydrogen tetrachloroaurate(III) trihydrate ($HAuCl_4$), silver nitrate ($AgNO_3$), and SDS, all AR-grade obtained from Sigma–Aldrich, were used as such without further purification. The double-distilled water was used for all sample preparations.

Synthesis of Zein Nanocubes. Synthesis of zein nanocubes was carried out by two methods. The first one is the in situ method where no external reducing or stabilizing agents were used and zein initiated the reduction as well as provided the colloidal stability. By doing so, zein prompted the protein–protein interactions to self-assemble in the form of nanocubes.

DOI: 10.1021/acsomega.8b02086
ACS Omega 2018, 3, 10851−10857

In the second method, we used the seed-growth (S-G) method,[18,19] where seeds grow into NPs while simultaneously allowing adsorption of zein on different crystal planes of NPs that subsequently derived the seeding process of protein to form self-assembled zein nanocubes.

In Situ Synthesis. In a round-bottom flask, 10 mL of (0.1, 0.2, and 0.4%) zein (dissolved in a specified amount of SDS aqueous solution) was taken along with $AgNO_3$. The mixture was shaken thoroughly for some time and kept in a thermostat bath at constant 80 °C for 24 h. Zein initiated the reduction and converted Ag(I) into Ag(0) with final pink to purple or yellow-brown color.[11] As soon as the Ag nucleating centers were created, zein stabilized them by surface adsorption and limiting growth proceeded to form tiny Ag NPs. The following reaction is expected to take place within first few hours of the reaction. This is followed by the protein−protein interactions

$$Ag^{+}(aq) + \text{zein protein (aq)} + e^{-} \rightarrow Ag^{0}(s) + \text{oxidizing products}$$

triggered by the surface-adsorbed protein that eventually self-assembled in the form of nanocubes. The samples were kept overnight and purified by centrifugation at 11 000 rpm after washing couple of times with double-distilled water.

Seed-Growth (S-G) Method. In this method, first of all Au seeds were prepared by mixing solutions of 1 mM trisodium citrate and 1 mM $HAuCl_4$ followed by an addition of an ice cold 0.5 mL (0.1 M) sodium borohydride solution. The red color confirms the formation of tiny Au seeds (Supporting Information, Figure S1), which were further used in the growth process. The growth of seeds into NPs was initiated by taking required amount of Au seeds in 10 mL of zein solution (0.1 and 0.2%) in the presence of $AgNO_3$ (0.25−1 mM) at 80 °C for 24 h. This reaction allowed the reduction of Ag(I) into Ag(0) by zein, and Ag atoms thus-created instantaneously nucleated on already present Au seeds in the solution. Similar reactions were also performed by taking Ag seeds (Figure S2) instead of Au seeds. The NPs thus-produced catalyzed the adsorption of zein to initiate protein−protein interactions that resulted in the self-assembled morphologies of zein. The purification of self-assembled morphologies of zein was carried out as mentioned in the previous method.

Instrumentation. The shape and size of zein self-assembled morphologies were determined with the help of TEM analysis performed on JEOL-2100 TEM, Japan. The sample was prepared by placing a drop of suspension on carbon-coated copper grid, dried in air, and analyzed at an operation voltage of 200 keV. Field-emission SEM analysis was done on Carl Zeiss Supra 55 at an operating voltage 10 keV for SEM images and 20 keV for EDX. Sample was prepared by placing the suspension on a glass substrate and analyzed after silver coating. XRD analysis was done on Shimadzu Maxima-X XRD, Japan. Sample was prepared by placing a drop of sample suspension on the glass substrate and dried in air. XRD patterns were collected at a wavelength of 1.54 Å (Cu Kα), an operating voltage of 40 keV, and a scan speed of 4° per min. Origin 6.1 and KaleidaGraph 3.5 were used to process and plot the spectra.

■ ASSOCIATED CONTENT

Supporting Information

The Supporting Information is available free of charge on the ACS Publications website at DOI: 10.1021/acsomega.8b02086.

TEM and SEM images of the samples and zeta potential measurements of the samples (PDF)

■ AUTHOR INFORMATION

Corresponding Author

*E-mail: bakshim@uwgb.edu.

ORCID

Mandeep Singh Bakshi: 0000-0003-1251-9590

Notes

The authors declare no competing financial interest.

■ ACKNOWLEDGMENTS

These studies were supported by start up funds from UWGB.

■ REFERENCES

(1) Bonneté, F. Colloidal Approach Analysis of the Marseille Protein Crystallization Database for Protein Crystallization Strategies. *Cryst. Growth Des.* **2007**, *7*, 2176−2181.

(2) Pusey, M. L.; Paley, M. S.; Turner, M. B.; Rogers, R. D. Protein Crystallization Using Room Temperature Ionic Liquids. *Cryst. Growth Des.* **2007**, *7*, 787−793.

(3) Yan, E.-K.; Zhao, F.-Z.; Zhang, C.-Y.; Yang, X.-Z.; Shi, M.; He, J.; Liu, Y.-L.; Liu, Y.; Hou, H.; Yin, D.-C. Seeding Protein Crystallization With Cross-Linked Protein Crystals. *Cryst. Growth Des.* **2018**, *18*, 1090−1100.

(4) Ribeiro, D.; Kulakova, A.; Quaresma, P.; Pereira, E.; Bonifácio, C.; Romão, M. J.; Franco, R.; Carvalho, A. L. Use of Gold Nanoparticles As Additives in Protein Crystallization. *Cryst. Growth Des.* **2014**, *14*, 222−227.

(5) Ko, S.; Kim, H. Y.; Choi, I.; Choe, J. Gold Nanoparticles As Nucleation-Inducing Reagents for Protein Crystallization. *Cryst. Growth Des.* **2017**, *17*, 497−503.

(6) Chen, Y.-W.; Lee, C.-H.; Wang, Y.-L.; Li, T.-L.; Chang, H.-C. Nanodiamonds As Nucleating Agents for Protein Crystallization. *Langmuir* **2017**, *33*, 6521−6527.

(7) Lee, S.-Y.; Gao, X.; Matsui, H. Biomimetic and Aggregation-Driven Crystallization Route for Room-Temperature Material Synthesis: Growth of β-Ga2O3Nanoparticles on Peptide Assemblies as Nanoreactors. *J. Am. Chem. Soc.* **2007**, *129*, 2954−2958.

(8) Bakshi, M. S. Nanoshape Control Tendency of Phospholipids and Proteins: Protein-Nanoparticle Composites, Seeding, Self-Aggregation, and Their Applications in Bionanotechnology and Nanotoxicology. *J. Phys. Chem. C* **2011**, *115*, 13947−13960.

(9) Mahal, A.; Tandon, L.; Khullar, P.; Ahluwalia, G. K.; Bakshi, M. S. PH Responsive Bioactive Lead Sulfide Nanomaterials: Protein Induced Morphology Control, Bioapplicability, and Bioextraction of Nanomaterials. *ACS Sustainable Chem. Eng.* **2017**, *5*, 119−132.

(10) Mahal, A.; Khullar, P.; Kumar, H.; Kaur, G.; Singh, N.; Jelokhani-Niaraki, M.; Bakshi, M. S. Green Chemistry of Zein Protein Toward the Synthesis of Bioconjugated Nanoparticles: Understanding Unfolding, Fusogenic Behavior, and Hemolysis. *ACS Sustainable Chem. Eng.* **2013**, *1*, 627−639.

(11) Navdeep; Banipal, T. S.; Kaur, G.; Bakshi, M. S. Nanoparticle Surface Specific Adsorption of Zein and Its Self-assembled Behavior of Nanocubes Formation in Relation to On-Off SERS: Understanding Morphology Control of Protein Aggregates. *J. Agric. Food Chem.* **2016**, *64*, 596−607.

(12) Piella, J.; Bastús, N. G.; Puntes, V. Size-Dependent Protein-Nanoparticle Interactions in Citrate-Stabilized Gold Nanoparticles:

DOI: 10.1021/acsomega.8b02086
ACS Omega 2018, 3, 10851−10857

The Emergence of the Protein Corona. *Bioconjugate Chem.* **2017**, *28*, 88−97.
(13) Vangala, K.; Siriwardana, K.; Vasquez, E. S.; Xin, Y.; Pittman, C. U.; Walters, K. B.; Zhang, D. Simultaneous and Sequential Protein and Organothiol Interactions With Gold Nanoparticles. *J. Phys. Chem. C* **2013**, *117*, 1366−1374.
(14) Thompson, A. B.; Calhoun, A. K.; Smagghe, B. J.; Stevens, M. D.; Wotkowicz, M. T.; Hatziioannou, V. M.; Bamdad, C. A Gold Nanoparticle Platform for Protein-Protein Interactions and Drug Discovery. *ACS Appl. Mater. Interfaces* **2011**, *3*, 2979−2987.
(15) Wu, S.; Myers, D. J.; Johnson, L. A. Factors Affecting Yield and Composition of Zein Extracted from Commercial Corn Gluten Meal. *Cereal Chem.* **1997**, *74*, 258−263.
(16) Pomes, A. F. Zein. In *Encyclopedia of Polymer Science and Technology: Plastics, Resins, Rubbers, Fibers*; Mark, H. F., Gaylord, N. G., Bikales, N. M., Eds.; Interscience Publishers: New York, 1971; Vol. *15*, pp 125−132.
(17) Esen, A. A proposed nomenclature for the alcohol-soluble proteins (zeins) of maize (Zea mays L.). *J. Cereal Sci.* **1987**, *5*, 117−128.
(18) Bakshi, M. S. How Surfactants Control Crystal Growth of Nanomaterials. *Cryst. Growth Des.* **2016**, *16*, 1104−1133.
(19) Bakshi, M. S. A Simple Method of Superlattice Formation: Step-by-Step Evaluation of Crystal Growth of Gold Nanoparticles through Seed−Growth Method. *Langmuir* **2009**, *25*, 12697−12705.
(20) Bakshi, M. S.; Possmayer, F.; Petersen, N. O. Role of Different Phospholipids in the Synthesis of Pearl-Necklace-Type Gold−Silver Bimetallic Nanoparticles as Bioconjugate Materials. *J. Phys. Chem. C* **2007**, *111*, 14113−14124.
(21) Ruiz-Morales, Y.; Romero-Martínez, A. Coarse-Grain Molecular Dynamics Simulations To Investigate the Bulk Viscosity and Critical Micelle Concentration of the Ionic Surfactant Sodium Dodecyl Sulfate (SDS) in Aqueous Solution. *J. Phys. Chem. B* **2018**, *122*, 3931−3943.
(22) Deo, N.; Jockusch, S.; Turro, N. J.; Somasundaran, P. Surfactant Interactions With Zein Protein. *Langmuir* **2003**, *19*, 5083−5088.
(23) Mallin, M. P.; Murphy, C. J. Solution-Phase Synthesis of Sub-10 nm Au−Ag Alloy Nanoparticles. *Nano Lett.* **2002**, *2*, 1235−1237.
(24) Murphy, C. J.; Gole, A. M.; Hunyadi, S. E.; Orendorff, C. J. One-Dimensional Colloidal Gold and Silver Nanostructures. *Inorg. Chem.* **2006**, *45*, 7544−7554.
(25) Yen, C.-W.; Lin, M.-L.; Wang, A.; Chen, S.-A.; Chen, J.-M.; Mou, C.-Y. CO Oxidation Catalyzed by Au−Ag Bimetallic Nanoparticles Supported in Mesoporous Silica. *J. Phys. Chem. C* **2009**, *113*, 17831−17839.
(26) Sasirekha, N.; Sangeetha, P.; Chen, Y.-W. Bimetallic Au-Ag/CeO2 Catalysts for Preferential Oxidation of CO in Hydrogen-Rich Stream: Effect of Calcination Temperature. *J. Phys. Chem. C* **2014**, *118*, 15226−15233.
(27) Otto, K.; Acik, I. O.; Krunks, M.; Tõnsuaadu, K.; Mere, A. Thermal decomposition study of HAuCl4·3H2O and AgNO3 as precursors for plasmonic metal nanoparticles. *J. Therm. Anal. Calorim.* **2014**, *118*, 1065−1072.
(28) Yang, Y.; Zhao, Y.; Yan, Y.; Wang, Y.; Guo, C.; Zhang, J. Preparation of AgCl Nanocubes and Their Application As Efficient Photoinitiators in the Polymerization of N-Isopropylacrylamide. *J. Phys. Chem. B* **2015**, *119*, 14807−14813.
(29) An, C.; Wang, R.; Wang, S.; Zhang, X. Converting AgCl nanocubes to sunlight-driven plasmonic AgCl : Ag nanophotocatalyst with high activity and durability. *J. Mater. Chem.* **2011**, *21*, 11532−11536.
(30) An, C.; Peng, S.; Sun, Y. Facile Synthesis of Sunlight-Driven AgCl:Ag Plasmonic Nanophotocatalyst. *Adv. Mater.* **2010**, *22*, 2570−2574.
(31) Iori, F.; Corni, S.; Di Felice, R. Unraveling the Interaction Between Histidine Side Chain and the Au(111) Surface: A DFT Study. *J. Phys. Chem. C* **2008**, *112*, 13540−13545.
(32) Wackerbarth, H.; Tofteng, A. P.; Jensen, K. J.; Chorkendorff, I.; Ulstrup, J. Hierarchical Self-Assembly of Designed 2 × 2-α-Helix Bundle Proteins on Au(111) Surfaces. *Langmuir* **2006**, *22*, 6661−6667.
(33) Di Felice, R.; Selloni, A.; Molinari, E. DFT Study of Cysteine Adsorption on Au(111). *J. Phys. Chem. B* **2003**, *107*, 1151−1156.
(34) Woods, K. E.; Perera, Y. R.; Davidson, M. B.; Wilks, C. A.; Yadav, D. K.; Fitzkee, N. C. Understanding Protein Structure Deformation on the Surface of Gold Nanoparticles of Varying Size. *J. Phys. Chem. C* **2016**, *120*, 27944−27953.
(35) Dominguez-Medina, S.; Kisley, L.; Tauzin, L. J.; Hoggard, A.; Shuang, B.; Indrasekara, A. S. D. S.; Chen, S.; Wang, L.-Y.; Derry, P. J.; Liopo, A.; Zubarev, E. R.; Landes, C. F.; Link, S. Adsorption and Unfolding of a Single Protein Triggers Nanoparticle Aggregation. *ACS Nano* **2016**, *10*, 2103−2112.
(36) Sun, J.; Wang, J.; Zhang, Y.; Wan, P.; Luo, L.; Wang, F.; Sun, X. Shape Evolution of Au Nanoring@Ag Core-Shell Nanostructures: Diversity From a Sole Seed. *Dalton Trans.* **2014**, *43*, 12495−12500.
(37) Ma, Y.; Xu, L.; Chen, W.; Zou, C.; Yang, Y.; Zhang, L.; Huang, S. Evolution From Small Sized Au Nanoparticles to Hollow Pt/Au Nanostructures With Pt Nanorods and a Mechanistic Study. *RSC Adv.* **2015**, *5*, 103797−103802.
(38) Li, L.; Chen, S.; Zheng, J.; Ratner, B. D.; Jiang, S. Protein Adsorption on Oligo(ethylene glycol)-Terminated Alkanethiolate Self-Assembled Monolayers: The Molecular Basis for Nonfouling Behavior. *J. Phys. Chem. B* **2005**, *109*, 2934−2941.
(39) Wackerbarth, H.; Tofteng, A. P.; Jensen, K. J.; Chorkendorff, I.; Ulstrup, J. Hierarchical Self-Assembly of Designed 2 × 2-α-Helix Bundle Proteins on Au(111) Surfaces. *Langmuir* **2006**, *22*, 6661−6667.
(40) Kalashnyk, N.; Nielsen, J. T.; Nielsen, E. H.; Skrydstrup, T.; Otzen, D. E.; Lægsgaard, E.; Wang, C.; Besenbacher, F.; Nielsen, N. C.; Linderoth, T. R. Scanning Tunneling Microscopy Reveals Single-Molecule Insights into the Self-Assembly of Amyloid Fibrils. *ACS Nano* **2012**, *6*, 6882−6889.
(41) Zhang, D.; Neumann, O.; Wang, H.; Yuwono, V. M.; Barhoumi, A.; Perham, M.; Hartgerink, J. D.; Wittung-Stafshede, P.; Halas, N. J. Gold Nanoparticles Can Induce the Formation of Protein-Based Aggregates at Physiological PH. *Nano Lett.* **2009**, *9*, 666−671.
(42) Chen, J.; Klem, S.; Jones, A. K.; Orr, B.; Holl, M. M. B. Folate-Binding Protein Self-Aggregation Drives Agglomeration of Folic Acid Targeted Iron Oxide Nanoparticles. *Bioconjugate Chem.* **2017**, *28*, 81−87.
(43) Yang, T.; Li, Z.; Wang, L.; Guo, C.; Sun, Y. Synthesis, Characterization, and Self-Assembly of Protein Lysozyme Monolayer-Stabilized Gold Nanoparticles. *Langmuir* **2007**, *23*, 10533−10538.

DOI: 10.1021/acsomega.8b02086
ACS Omega 2018, 3, 10851−10857